



# Strain and Thermal Effects on Magnetic Hysteresis of a Modified JA-SW Model

Zizheng Guo<sup>a\*</sup>, Chudong Xu<sup>b</sup>, Weiqing Jia<sup>c</sup>, Jun Liu<sup>d</sup>

<sup>a\*,b,c,d</sup>Department of Applied Physics, College of Electronic Engineering, South China Agricultural University, Guangzhou, China

**Abstract:** The JA (Jiles-Atherton) - SW(Stoner-Wohlfarth) model is extended to include the strain or stress anisotropy. With the improved model, the strain and thermal effects on magnetic hysteresis loss are studied. Interesting results are shown in two aspects. Firstly, a transition-like behavior is found for the temperature dependent hysteresis loss (or more precisely, the hysteresis curve area). Secondly, as the magnitude of strain anisotropy increases, the hysteresis loss decreases initially and then increases, resulting in a valley structure of the curve of the strain dependent hysteresis loss. The results are compared with those of literature and the differences between them are discussed.

**Keywords:** Magnetic Films and Multilayers; Magnetic Hysteresis Model; Strain; Temperature.

## 1. Introduction

Hysteretic phenomena are encountered in many different areas of science and engineering, including magnetic materials, piezoelectric and piezoceramic actuators shape memory alloys, superconductor, mechanical and optical systems and others. In order to give a complete understanding of the hysteretic phenomena, many physical and mathematical models about hysteresis were proposed and have been fully discussed. Generally, hysteresis models can be divided into two kinds: semi-physical and physical ones. The physical models, such as the Maxwell model and the Jiles-Atherton (JA) model [1] are refined based on physical phenomena or specific physical problems. The semi-physical models are phenomenological models, mainly including the Bouc-Wen model [2], the Preisach model [3], the neural network model, etc.

In general, the magnetic field is vectorial, and the magnetization process in magnetic materials has to be considered using vector magnetization. Thus, the magnetization of materials must be treated as a vector with magnitude and direction. Unfortunately, all of the above hysteresis models are scalar ones. It is the scalar characteristics that limit their applications. For example, the JA model is currently widely used in simulations and device designs, mainly due to its implementation simplicity in fast and stable algorithms, but the JA model is a scalar and isotropic one-it does not include anisotropy that affects severely hysteretic properties of single-domain, thin-film devices. On the other hand, the Stoner-Wohlfarth (SW) model [4] can well describe the anisotropy but does not account for dynamic response and incremental energy loss. Therefore, it is a natural consideration that one can improve the scalar models by combining them with the SW model. The first work was done by Dimitropoulos et al. [5] in 2006 and their model was called the JA-SW hybrid model. With this three-dimensional (3-D) vector model, one can handle anisotropy problems very convenient.

Recently, strain or stress effects are considered important for ferromagnetic film systems, especially for magnetostrictive materials (such as terfenol-D). How to describe the strain effects in hysteresis models is very attractive. The basic idea to solve this problem is still through the improvement of the JA model. In the literature [6], [7], [8], [9], [10], a strain field was added into the effective field, in this way the stress or strain caused by elastic deformation can be included in the JA model. However, these modified models are still scalar ones. In order to make them vectorial, a combination with other vector models (*e.g.*, the SW model) is needed once again. We have noted that, in some SW-like models, two kinds of different anisotropy can be merged together by means of mathematical transformations [11], [12]. Based on this

technique, we can merge the strain anisotropy into the uniaxial anisotropy term used in the JA-SW hybrid model mentioned above. In this way, we make an improvement for the JA-SW hybrid model. We will call this new model the JA-SW strain model and use it to discuss the strain effects on magnetic hysteresis.

For a long time, hysteresis loss is an interesting issue for scientists of many fields. In this paper, we will focus our attention on the strain and temperature effects on hysteresis loss. To our knowledge, characteristics of hysteresis loss due to stress or strain effects have not been investigated except in few reports. Yamamoto et al. [13] studied the effect of compressive stress on hysteresis loss of Terfenol-D and found that the area of the hysteresis loop, i.e. hysteresis loss, monotonically increased as stress was increased. However, further investigations showed complex behaviors of the strain (stress) dependent hysteresis loss curves. In details, it was found that there exists a small range for small stress where the hysteresis loss decreases first and then increases in the process of stress increasing [14], [15]. Thus, this situation requires further clarification, which is the subject of this paper.

Zhu, et al. [16] Studied the temperature dependence of the hysteresis loss of the Icing model and found a transition-like behavior of the hysteresis loop area. Since then, many authors published their papers which attempted to make sure that if this is the general phenomenon of the cooperative many-body systems [17], [18], [19]. In this paper, we will do further investigation on this issue. We will use our JA-SW strain model to study both the strain and thermal effects of the magnetic hysteresis loss.

## 2. The JA-SW Hybrid Model

According to the JA model, the total magnetization of a ferromagnetic material can be represented as the sum of contributions of irreversible,  $\vec{M}_{ir}$ , and reversible,  $\vec{M}_{re}$ , magnetization components

$$\vec{M} = \vec{M}_{re} + \vec{M}_{ir} \quad (1)$$

Or

$$\vec{M} = c\vec{M}_{ir} + (1-c)\vec{M}_{an} \quad (2)$$

With  $c$  the reversibility coefficient and  $\vec{M}_{an}$  is the anhysteretic magnetization

Irreversible magnetization component  $\vec{M}_{ir}$  is determined by

$$\dot{\vec{M}}_{ir} = \begin{cases} \left[ -\frac{k_0}{2k_1} + \sqrt{\frac{k_0^2}{4k_1^2} + \frac{\vec{M}_{an} - \vec{M}_{ir}}{k_1} \cdot \dot{\vec{H}}_E u((\vec{M}_{an} - \vec{M}_{ir}) \cdot \dot{\vec{H}}_E)} \right] \frac{\vec{M}_{an} - \vec{M}_{ir}}{|\vec{M}_{an} - \vec{M}_{ir}|} (k_1 \neq 0) \\ \frac{\vec{M}_{an} - \vec{M}_{ir}}{k_0} \cdot \dot{\vec{H}}_E u((\vec{M}_{an} - \vec{M}_{ir}) \cdot \dot{\vec{H}}_E) \frac{\vec{M}_{an} - \vec{M}_{ir}}{|\vec{M}_{an} - \vec{M}_{ir}|} (k_1 = 0) \end{cases} \quad (3)$$

$$\vec{M}_{ir} = 0 (k_1 = k_0 = 0)$$

in which  $\dot{\vec{M}}_{ir} = \frac{d\vec{M}_{ir}}{dt}$ ,  $\dot{\vec{H}}_E = \frac{d\vec{H}_E}{dt}$ , parameter  $k$  is called the pinning constant, and  $k = k_0 + k_1 \left| \dot{\vec{M}} \right|$ , with

$\dot{\vec{M}} = \frac{d\vec{M}}{dt}$ .  $u(x) = \begin{cases} 1 & \text{for } x \geq 0 \\ 0 & \text{for } x < 0 \end{cases}$  is the unit-step function. The anhysteretic magnetization

$\vec{M}_{an}$  is calculated by

$$\vec{M}_{an} = L\left(\left|\vec{H}_E + \vec{H}_F\right|\right) \frac{\vec{H}_E + \vec{H}_F}{\left|\vec{H}_E + \vec{H}_F\right|} = M_s \frac{\beta \left|\vec{H}_E + \vec{H}_F\right|}{1 + \beta \left|\vec{H}_E + \vec{H}_F\right|} \frac{\vec{H}_E + \vec{H}_F}{\left|\vec{H}_E + \vec{H}_F\right|} \quad (4)$$

With  $M_s$  the saturation magnetization.  $L()$  stands for the Langevin function, in which constant  $\beta \propto 1/T$ , with  $T$  the temperature.

$$\vec{H}_E = \vec{H} + \alpha \vec{M} \quad (5)$$

Is the effective field taking into account the domain interactions,  $\alpha$  is the molecular field parameter.

$$\vec{H}_F = \frac{2K_u}{M_s^2} (\vec{M}_{an} \cdot \hat{e}_u) \hat{e}_u \quad (6)$$

Is obtained from the SW model

$$E_u = -K_u \cos^2(\phi) \quad (7)$$

With  $K_u$  the anisotropy constant,  $\phi$  is the angle made by  $\vec{M}_{an}$  with the direction of easy axis (EA),  $\hat{e}_u = [\cos\phi, \sin\phi, 0]$  is the unit vector in the direction of EA (A detailed description for the Eqs. (1)-(7) can be found in Ref.[5]).

### 3. The JA-SW Strain Model

Take the ferromagnetic (FM)/antiferromagnetic(AFM) bilayer as an example of the single domain systems. In this case,  $\phi$  is the orientation angle of the FM magnetization to the FM EA,  $K_u$  the uniaxial anisotropy constant of the FM layer. The external field is applied parallel to the easy axis (EA) in the film plane. The anisotropy energy of the AFM layer is neglected. We consider only in-plane stress, with  $\sigma$  the mechanical stress vector directed at angle  $\psi$  to the direction of EA. The magneto-elastic free energy is determined by the saturation magnetostriction coefficient  $\lambda_s$ . In this paper, we do not consider the sign of the magnetostriction coefficient of the material,  $\lambda_s$ , and do not consider the external stress is positive or negative (tensile or compressive). We just focus on the case that  $\lambda_s\sigma > 0$ . If we are making the notations  $K_\sigma = \frac{3\lambda_s\sigma}{2M_s}$ , the total free energy density may be rewritten in the reduced form, as:

$$E = E_u + E_\sigma = -K_u \cos^2 \phi - K_\sigma \cos^2(\psi - \phi). \quad (8)$$

If one chooses  $\tan 2\phi_0 = \frac{K_\sigma \sin 2\psi}{K_u + K_\sigma \cos 2\psi}$ , Eq. (8) may be transformed into [11],[12]

$$E = -K_u^* \cos^2(\phi^*) + K_u^* \sin^2 \phi_0 - K_\sigma \sin^2 \psi, \quad (9)$$

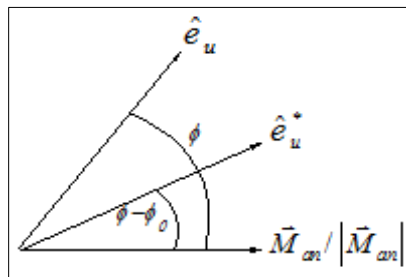
where

$$K_u^* = \sqrt{K_u^2 + K_\sigma^2 + 2K_u K_\sigma \cos(2\psi)} \quad (10)$$

is an equivalent total anisotropy field and  $\phi^* = \phi - \phi_0$  is the angle between this equivalent total anisotropy field and  $\vec{M}_{an}$  and  $\hat{e}_u^* = [\cos\phi^*, \sin\phi^*, 0] = [\cos(\phi - \phi_0), \sin(\phi - \phi_0), 0]$  called the unit vector in the direction of effective EA. A schematic illustration for the direction of  $\hat{e}_u^*$  and its relation with  $\hat{e}_u$  is illustrated in Fig.1.

Replacing  $K_u$  with  $K_u^*$  and  $\hat{e}_u$  with  $\hat{e}_u^*$  in Eqs.(1)-(6) leads to a modified JA-SW strain model.

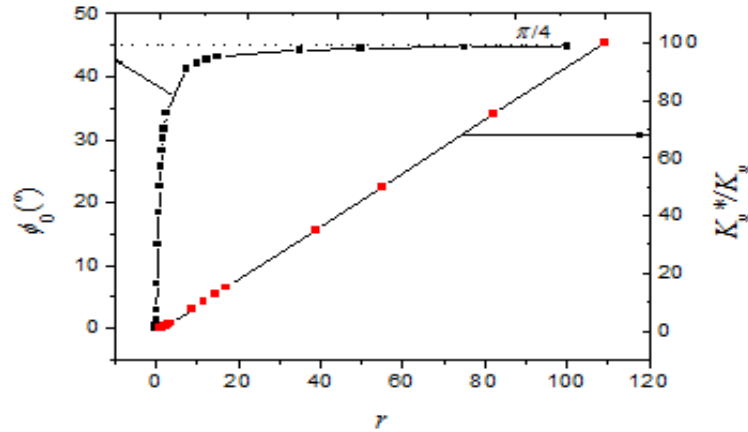
**Figure 1.** Schematic illustration for the direction of the effective anisotropy



Source: Author

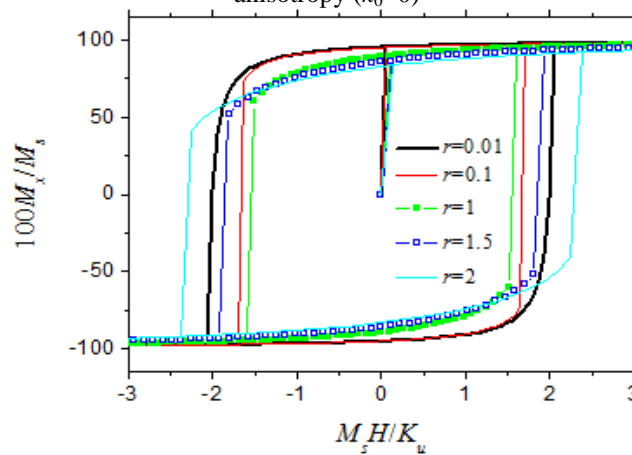
Taking  $\psi=45^\circ$  (corresponding to the biaxial in-plane strain caused by lattice mismatch) and letting  $r=K_\sigma/K_u$  result in  $\phi_0 = (1/2) \tan^{-1} r$  and  $K_u^* = K_u \sqrt{1+r^2}$ . Obviously, when  $r \rightarrow \infty$ ,  $\phi_0 \rightarrow \pi/4$ ; and when  $r \ll 1$ ,  $K_u^* = rK_u$ . Detailed properties of these two quantities can be seen from Fig.2.

**Figure 2.**  $\phi_0$  and the magnitude of effective anisotropy vs. the magnitude of strain anisotropy



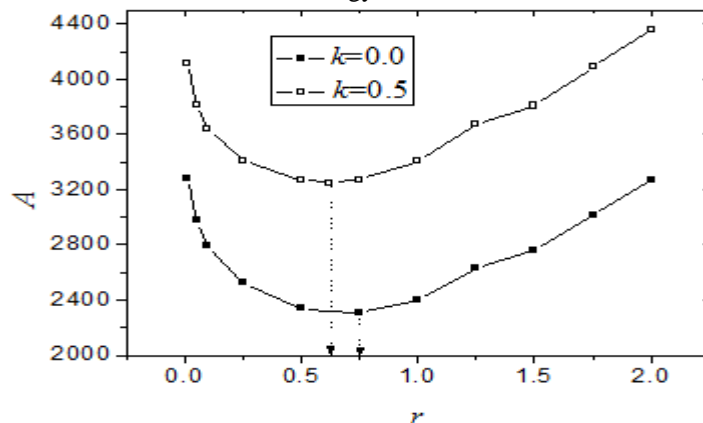
Source: Author

**Figure 3.** Hysteresis curves for the case with no incremental energy loss and for different magnitudes of strain anisotropy ( $k_0=0$ )



Source: Author

**Figure 4:** Variation of hysteresis loop area  $A$  (in units of  $K_u$ ) with  $r$ , for the cases with and without incremental energy loss



Source: Author

The hysteresis curves for the case with no incremental energy loss and for different magnitudes of strain anisotropy are presented in Fig. 3 ,in which we have defined  $\hat{e}_x=[1,0,0]$  and  $M_x=\vec{M} \cdot \hat{e}_x$ ,  $H=|\vec{H}|$ . Other parameters employed are  $\beta=10$ ,  $M_s=100$ ,  $\hat{e}_u=[1,0,0](\phi=0^\circ)$ ,  $k_1=\alpha=0$ ,  $K_u=100$ . From these hysteresis loops, we can obtain the hysteresis losses (defined as the hysteresis loop area) easily.

Fig.4 shows the variation of hysteresis loop area  $A$  (in units of  $K_u$ ) with  $r$ . It is easy to understand that the hysteresis loss increases when considering of the contribution of the incremental energy loss.

In the above calculation, we have used the range of  $r$  from 0.01 to 2.0. In fact, this range is of practical meaning. In Ref. [20],  $\text{CoFe}_2\text{O}_4$  film was fabricated on  $\text{SrTiO}_3$  substrate, their lattice constants are  $8.392 \text{ \AA}$  ( $a_F$ ) and  $3.905 \text{ \AA}$  ( $a_s$ ), respectively. With parameters  $\lambda_s=-590 \times 10^{-6}$ ,  $Y=1.5 \times 10^{12} \text{ dyn/cm}^2$ , and  $K_u=3 \times 10^6 \text{ erg/cm}^3$ , we can estimate the magnitude of the stress anisotropy of the stress

induced anisotropy field from  $K_\sigma = \frac{3\lambda_s\sigma}{2M_s} = \frac{3\lambda_s Y \varepsilon}{2M_s}$  ( $\varepsilon = \left| \frac{a_s - a_F}{a_F} \right|$  is the lattice mismatch) as

$K_\sigma = 3.2 \times 10^6 \text{ erg/cm}^3$ , which is on the same order as  $K_u$ . Under this condition,  $r=K_\sigma/K_u \approx 1.0$ .

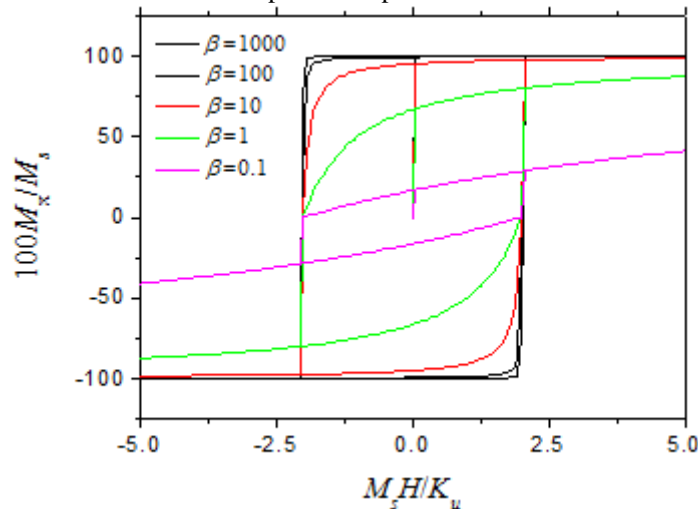
It is interesting that the curves show minimums which shift left when  $k_0$  is increased. In details, there exists a small range of stress where the hysteresis loss decreases initially and then increases as stress is increased. This phenomenon was also found in Ref.[14]. In Ref.[15], the coercivity showed similar behavior. Since  $A$  is proportional to coercivity, the origins of the valley phenomena of hysteresis loss and coercivity may be the same. In order to understand this phenomenon better, we have carried out several numerical experiments. It is shown that this phenomenon is determined by both  $K_u^*$  and  $\hat{e}_u^*$ , and it can be attributed to the inherent nonlinearity of the JA Model. In the above calculations, we have limited to the case  $\phi=0^\circ$ . When  $\phi=90^\circ$ , similar trends of the curves could be found.

At last, we do some comparison for some JA based hysteresis models related with stress or strain. Refs. [6-10] made incorporation of stress through the effective field, *i.e.*, modified Eq.(5) by  $\vec{H}_E = \vec{H} + \hat{\alpha} \vec{M}$ , with the parameter  $\hat{\alpha}$  for quantifying magnetic and stress interactions. But, as such, the improved models are still scalar models instead of vector ones.

#### 4. Temperature Dependence of Hysteresis Loss

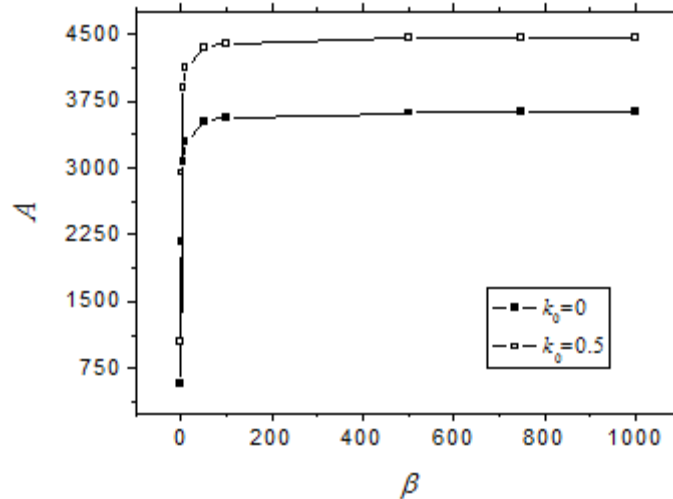
To simplify the calculation, we take  $r=0$  throughout this section. In this case, our model reduces to that of Ref.[5]. Employed parameters are  $M_s=100$ ,  $\hat{e}_u=[1,0,0]$ ,  $k_1=\alpha=0$ ,  $K_u=100$ .

**Figure 5.** Hysteresis curves for different reciprocal temperatures and with no incremental energy loss ( $k_0=0$ )



Source: Author

**Figure 6.** Variation of hysteresis loop area  $A$  (in units of  $K_u$ ) with  $\beta$  (reciprocal temperature), for the cases with and without incremental energy loss



Source: Author

The Hysteresis curves for the case with no incremental energy loss and for different reciprocal temperatures are depicted in Fig. 5, in which the variables are defined as in Fig.3. Fig.6 shows the variation of hysteresis loop area  $A$  (in units of  $K_u$ ) with  $\beta$ . Similar to Fig.4, the hysteresis curve area  $A$  increases when considering of the contribution of the incremental energy loss.

The temperature dependent trend of the JA-SW model is in accordance with Ref. [17], but in contrast with Ref. [18]. The difference between them maybe lie in the limitations of the used models and detailed analysis of the thermal effects of hysteresis can be reached by considering the temperature

dependent parameters of the JA model[19]. In this way we can write  $M_s(T)=M_s^{Ta}(1-\exp\frac{T-T_c}{\tau_{M_s}})^{-1}$ , where

$M_s^{Ta}$  is the value of spontaneous magnetization at room temperature,  $T_c$  is the Curie temperature, and  $\tau_{M_s}$  is the constant defined on the experimental curve of spontaneous magnetization with temperature .Since the five parameters of the JA model are all related with  $M_s$ , they become temperature dependent. For

example, parameter  $\alpha$  is in the form of  $\alpha(T)=\alpha^{Ta}(1-\exp\frac{T-T_c}{\tau_{M_s}})^{-1}$ , where  $\alpha^{Ta}$  is the value of parameter  $\alpha$

at room temperature. From the expressions of  $M_s$  and the five parameters, we can know that the thermal behaviors would be different before and after the Cure temperature  $T_c$  and this effect cannot be shown in our above model.

## 5. Summary

In summary, the 3-D vector JA-SW model is extended to include the strain or stress anisotropy. This kind of anisotropy could come from applied stress or strain caused by lattice mismatch. With this improved model, a simulation is carried out to study the effects of strain and temperature on magnetic hysteresis loss. A transition-like behavior is found for the temperature dependent hysteresis loss (or, more precisely, the hysteresis curve area). As the magnitude of strain anisotropy increases, the hysteresis loss decreases initially and then increases and a minimum is shown in the curve of the strain dependent hysteresis loss. The simulation shows that the modified JA-SW strain model can describe the stress or strain anisotropy conveniently.

## Acknowledgements

Project supported by the Natural Science Foundation of Guangdong China (Grant No. 2015A030313400).

## References

- [1] P. Rasilo, D. Singh, D. Aydin, F. Martin, R. Kouhia, A. Belahcen, *et al.*, "Modeling of hysteresis losses in ferromagnetic laminations under mechanical stress," *IEEE Transactions on Magnetics*, vol. 52, pp. 1-4, 2016.
- [2] M. Ismail, F. Ikhouane, and J. Rodellar, "The hysteresis bouc-wen model, a survey," *Archives of Computational Methods in Engineering*, vol. 16, pp. 161-188, 2009.
- [3] A. Kedous-Lebouc, A. Vernescu, and B. Cornut, "A two-dimensional Preisach particle for vectorial hysteresis modeling," *Journal of Magnetism & Magnetic Materials*, vol. 254-255, pp. 321-323, 2003.
- [4] E. C. Stoner and E. P. Wohlfarth, "mechanism of magnetic hysteresis in heterogeneous alloys," *IEEE Transactions on Magnetics*, vol. 27, pp. 3475-3518, 1948.
- [5] D. P. D., G. I. Stamoulis, and E. Hristoforou, "A 3-D hybrid Jiles-Atherton/Stoner-Wohlfarth magnetic hysteresis model for inductive sensors and actuators," *IEEE Sensors Journal*, vol. 6, pp. 721 -736, 2006.
- [6] J. Zheng, S. Cao, H. Wang, and W. Huang, "Hybrid genetic algorithms for parameter identification of a hysteresis model of magnetostrictive actuators," *Neurocomputing*, vol. 70, pp. 749-761, 2007.
- [7] W. Huang, B. Wang, S. Cao, Y. Sun, L. Weng, and H. Chen, "Dynamic Strain Model With Eddy Current Effects for Giant Magnetostrictive Transducer," in *IEEE Conference on Electromagnetic Field Computation*, 2006, p. 213.
- [8] S. Valadkhan, K. Morris, and A. Khajepour, "Review and comparison of hysteresis models for magnetostrictive materials," *Journal of Intelligent Material Systems & Structures*, vol. 20, pp. 131-142, 2008.
- [9] M. J. Sablik, S. Rios, F. J. G. Landgraf, T. Yonamine, and C. M. F. De, "Modeling of sharp change in magnetic hysteresis behavior of electrical steel at small plastic deformation," *Journal of Applied Physics*, vol. 97, p. 94, 2005.
- [10] M. J. Sablik, T. Yonamine, and F. J. G. Landgraf, "Modeling plastic deformation effects in steel on hysteresis loops with the same maximum flux density," *IEEE Transactions on Magnetics*, vol. 40, pp. 3219-3226, 2004.
- [11] Z. Z. Guo, "Angular dependences of the switching field and coercivity for magnetic multilayer films with strain caused by lattice mismatch," *Solid State Communications*, vol. 151, pp. 116-119, 2011.
- [12] Z. Z. Guo, "Origin of the cusp phenomenon in the coercivity curves of a stoner-wohlfarth magnet under stress," *International Journal of Modern Physics and Applications*, vol. 1, pp. 139-144, 2015.
- [13] K. Yamamoto, H. Nakano, and Y. Yamashiro, "Effect of compressive stress on hysteresis loss of Terfenol-D," *Journal of Magnetism & Magnetic Materials*, vol. 254-255, pp. 222-224, 2003.
- [14] K. Yamamoto and Y. Yamashiro, "Ken-ichi magnetic properties of non-oriented electrical steels under compressive stress normal to their surface," *Przegląd Elektrotechniczny*, vol. 87, pp. 97-100, 2011.
- [15] K. Yamamoto and Y. Yamashiro, "Effect of compressive stress on hysteresis loss and magnetostriction of grain oriented Si-Fe sheets," *Journal of Applied Physics*, vol. 93, pp. 6683-6685, 2003.
- [16] H. Zhu, S. Dong, and J. M. Liu, "Hysteresis loop area of the Ising model," *Physical Review B*, vol. 70, pp. 2806-2810, 2004.
- [17] A. Tamion, E. Bonet, F. Tournus, C. Raufast, A. Hillion, O. Gaier, *et al.*, "Efficient hysteresis loop simulations of nanoparticle assemblies beyond the uniaxial anisotropy," *Physical Review B*, vol. 85, pp. 1279-128, 2012.
- [18] H. Y. Lu, J. G. Zhu, and H. S. Y. Ron, "Measurement and modeling of thermal effects on magnetic hysteresis of soft ferrites," *IEEE Transactions on Magnetics*, vol. 43, pp. 3952-3960, 2007.
- [19] A. Ladjimi and M. R. Mékideche, "Modeling of thermal effects on magnetic hysteresis using the jiles-atherton model," *Przegląd Elektrotechniczny*, vol. 88, pp. 253-256, 2012.
- [20] P. D. Thang, G. Rijnders, and D. H. A. Blank, "Stress-induced magnetic anisotropy of CoFe<sub>2</sub>O<sub>4</sub> thin films using pulsed laser deposition," *Journal of Magnetism & Magnetic Materials*, p. 310, 2007.